ijmc

Simulation of Tetracycline onto Graphene Nano Sheet

Gh. Soleimani[a], E. Ezzatpour Ghadim[b], S. Kimiagar[a],*

[a]Department of Physics, Islamic Azad University, Central Tehran Branch (IAUCTB), Tehran, Iran.
[b]Young Researchers and Elite Club, Islamic Azad University, Central Tehran Branch (IAUCTB), Tehran, Iran

Abstract. Tetracycline (TC) is a broad spectrum of antibiotic which is used to cure infectious and cancer. It can cause harmful side effects due to its high absorption in all organs. On the other hand graphene is appropriate to carry drug and release it into special target, organ or cell. It may decrease the side effects of drug dramatically by using low dosage of medicine. Graphene sheet is able to adsorb molecules of TC via π-π stacking interaction. Base on this mechanism, simulation of TC molecule onto graphenenano sheets was adjusted. Study of force in the z direction illustrated that TC is closed to graphene via carbon (C_8) phenolic ring then rotates and it is again closed to graphene sheet from amino group side. This case is adsorption equilibrium and total energy of the system is -6800eV.

Index to information contained in this paper

1. Introduction

The first antibiotic was discovered in 1928 by Fleming who was awarded Nobel Prize. Accidentally he realized the antibacterial property of Penicilliumnotatum [1]. There are five basic mechanisms of antibiotic action against bacterial cells: inhibition of cell wall synthesis, inhibition of protein synthesis, alteration of cell membranes, inhibition of nucleic acid synthesis, anti-metabolite activity [2]. Some types of antibiotics can be referred to: Beta-lactams, tetracycline, erythromycin, clindamycin and streptomycin. The

---

*Corresponding author. Email: s.kimia8579@gmail.com

tetracycline is produced by soil microorganisms and is used to treat infectious diseases, bacterial and cancer treatment. It has many side effects such as other drugs [3, 6]. TC may cause stomach or bowel upsets, and, on rare occasions, allergic reactions [4]. Nano-particles are used as drug carriers to reduce the side effects of TC. Among different nano particles, graphene has an individual properties and applicable in drug delivery systems and biochemistry [5]. Graphene has honeycomb mono atomic layer which has manufactured by variety unsaturated C=C bond on the surface [7]. Graphene can absorb and release the molecule with aromatic and unsaturated structure via π-π interactions [8].Tetracycline structure with phenolic ring, π bond and amino group can interact with graphene aromatic groups by π bonds. It means TC molecules on graphene surface can represent an equilibrium concentration [9, 10].

LAMMPS is a classical molecular dynamics code that models an ensemble of particles in a liquid, solid, or gaseous state. It can model atomic, polymeric, biological, metallic, granular, and coarse-grained systems using a variety of force fields and boundary conditions. LAMMPS runs efficiently on single-processor desktop or laptop machines, but it designed for parallel computers. It can model systems with only a few particles up to millions or billions. In the most general sense, LAMMPS integrates Newton's equations of motion for collections of atoms, molecules, or macroscopic particles that interact via short- or long-range forces with a variety of initial and/or boundary conditions. For computational efficiency LAMMPS uses neighbor lists to keep track of nearby particles. The lists are optimized for systems with particles that are repulsive at short distances, so that the local density of particles never becomes too large [11, 12].

In this study, we simulated TC molecule onto graphenenano sheet using molecular dynamics by Lammps. The result showed adsorption equilibrium of the TC molecule in the vicinity of graphene sheet.

2. Computational Model

For simulation, the structure of TC and graphene, potential between (C, C) atoms and (TC, C) atoms are needed. We clarify the potentials which have been used in our model. The airebo pair style computes the Adaptive Intermolecular Reactive Empirical Bond Order (AIREBO) Potential for a system of carbon and hydrogen atoms. The rebo pair style computes the Reactive Empirical Bond Order (REBO) Potential.

The AIREBO potential consists of three terms:

$$E = \frac{1}{2}\sum_i \sum_{i \neq j}\left[E_{ij}^{REBO} + E_{ij}^{LJ} + \sum_{k \neq i,j}\sum_{l \neq i.j.k} E_{kijl}^{TORSION}\right] \tag{1}$$

By default, all three terms are included. For the airebo style, if the two optional flag arguments to the pair style command are included, the LJ and torsional terms can be turned off. Note that both or neither of the flags must be included. If both of the LJ an torsional terms are turned off, it becomes the 2nd−generation REBO potential. The detailed formulas for this potential are given in [13]; here we provide only a brief description. The E_REBO term has the same functional form as the hydrocarbon REBO potential developed in [14]. The coefficients for E_REBO in AIREBO are essentially the same as Brenner's potential, but a few fitted spline values are slightly different. For most cases the E_REBO term in AIREBO will produce the same energies, forces and statistical averages as the original REBO potential from which it was derived. This potential is the developed form of Tersoff potential. The functional form of the Tersoff potential used in this work is

356

similar to worked by Smith [15], modified by Sayed et al [12]and is shown below:

$$E = \sum_i E_i = \frac{1}{2}(2) \tag{2}$$

$$V_{ij} = f_c(r_{ij})[V_R(r_{ij}) - b_{ij}V_A(r_{ij})] \tag{3}$$

$$f_c(r) = \begin{cases} 1 \, , \ r < (R - R_{cut}) \\ \frac{1}{2}\left[1 - sin\left[\frac{\pi(r-R)}{2R_{cut}}\right]\right] \, , \ R - R_{cut} < r < R + R_{cut} \\ 0 \, , \ r > (R + R_{cut}) \end{cases} \tag{4}$$

$$V_R(r_{ij}) = \left[\frac{D_e}{S-1}\right] exp\left(-\beta\sqrt{2S}(r_{ij} - r_e)\right) \tag{5}$$

$$V_A(r_{ij}) = \left[\frac{S\,D_e}{S-1}\right] exp\left(-\beta\sqrt{\frac{2}{S}}(r_{ij} - r_e)\right) \tag{6}$$

$$b_{ij} = \left[1 + (\gamma\xi_{ij})^n\right]^{-\frac{1}{2n}} \tag{7}$$

$$\xi_{ij} = \sum_{k \neq ij} f_c(r_{ik})g(\theta_{jik})\omega_{ik} \tag{8}$$

$$\omega_{ik} = exp\left[\lambda^3(r_{ij} - r_{ik})^3\right] \tag{9}$$

$$g(\theta_{jik}) = 1 + \left(\frac{c}{d}\right)^2 - \frac{c^2}{d^2 + (h - cos\,\theta_{jik})^2} \tag{10}$$

where, E is the total energy of the system of interest. E_i is the site energy of the atom labeled *i*. The indices *i, j* and *k* run over all of the atoms in the system.V_{ij} is the interaction energy and is based upon a combination of an exponential Morse-like pair potentials and is a function of r_{ij} , the physical distance between atoms *i* and *j*. V_A and V_R respectively provide the attractive and repulsive pair-potential parts of the interaction energy for the exponential Morse-like pair relating atom *i* and atom *j*. $f_c(r)$ provides a smooth spherical cut-off function around atom *i* based upon the distance to the first nearest-neighbor shell. Another form of the Tersoff potential [16] is specified in terms of the parameters A_{ij} , B_{ij} , λ_{ij} and μ_{ij} which are reproduced by many authors and generally labeled T3[17]. The conversion factors to produce the parameters of the form used here from the original Tersoff notation are:

$$S = \frac{\lambda}{\mu} \tag{11}$$

$$\beta = \frac{\lambda}{\sqrt{2S}} \tag{12}$$

$$r_e = \frac{In\frac{SA}{B}}{\beta\left(\sqrt{2S} - \sqrt{\frac{2}{S}}\right)} \tag{13}$$

$$D_e = A(S-1)exp\left[-\beta.r_e.\sqrt{2S}\right] \tag{14}$$

$$R_{cut} = \frac{S_{ij} - R_{ij}}{2} \tag{15}$$

357

$$R = R_{ij} + R_{cut} \tag{16}$$

To invert the parameters from this form back to the original Tersoff form we can use:

$$A = \frac{D_e}{S-1} exp[\beta.r_e.\sqrt{2S}] \tag{17}$$

$$B = \frac{SD_e}{S-1} exp\left[\beta.r_e.\sqrt{\frac{2}{S}}\right] \tag{18}$$

$$\lambda = \sqrt{2S} \tag{19}$$

$$\mu = \sqrt{\frac{2}{S}} \tag{20}$$

$$S_{ij} = R - R_{cut} \tag{21}$$

$$R_{ij} = R + R_{cut} \tag{22}$$

The value for R can be found by taking the distance vector to the nearest neighbor shell and the distance vector to the second nearest neighbor shell and averaging the result, hence:

$$R = \frac{r_{1nn}+r_{2nn}}{2} \tag{23}$$

For a variety of hydrocarbon materials, coefficients and specific constants has obtained which is called Brenner potential. The E_LJ term adds longer−ranged interactions and in AIREBO contains a series of switching functions so that the short−ranged LJ repulsion

($\frac{1}{r^{12}}$) does not interfere with the energetic captured by the E_REBO term [18].

$$U(r_{ij}) = 4\varepsilon\left[\left(\frac{\sigma}{r_{ij}}\right)^{12} - \left(\frac{\sigma}{r_{ij}}\right)^{6}\right] \tag{24}$$

where r_{ij} denotes the distance between the two particles *i* and *j*. The parameters ε and σ give the "hardness" and the scaling range of the potential.

The E_TORSION term is an explicit 4-body potential that describes various dihedral angle preferences in hydrocarbon configurations.
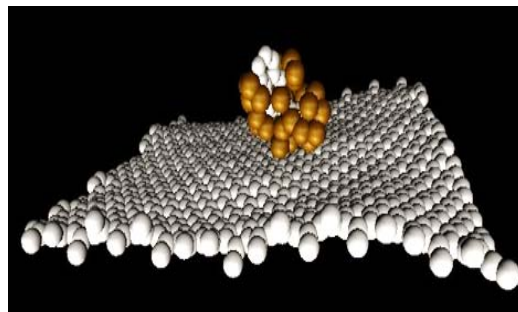

Figure 1:TC on grapheme nano sheet.

Graphene nano sheet with dimensions *25 × 25* nm in *XY* plane with *z=-5* and TC molecule at position (*x=0, y=0, z=0*) were considered (Figure 1). The cut of radius was 10 Å and periodic boundary condition was applied. During the first 1000 fs steps of simulation, temperature increased up to 25°C. After equilibrium state simulation continued up to 200000 fs steps and final data were extracted. For all atoms Z component and force were averaged.

3. Result and Discussion

Figure 2 shows the molecular structure of TC in which numbers 4 and 8 indicate the location of nitrogen from ammine and C_8 carbon, respectively. The Z component of TC molecule variation by time has shown in Figure 3. TC molecule closes to graphene sheet from C_8 carbon phenolic ring up to the 6.2 Å. When center of molecules is at 7 Å, it starts to rotate at 15000 fs. Then closes to graphene from ammine side up to 5 Å and at ~17000 fs goes far from graphene sheet.
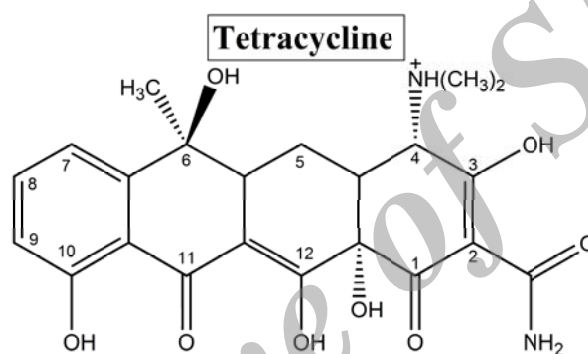

Figure 2: The TC molecular structure.

The square sign (Figure 3) refers to average of Z component. It is seen Z increases by time up to 16000 fs and then decreases.
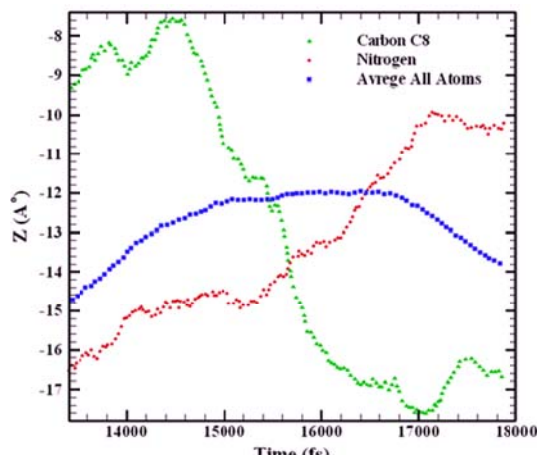
359

Figure 3: Z component of TC molecules.

Figure 4 shows three dimensional curve of variation of X and Z component by time. The rotating of TC molecule is recognizable. Summation of force vectors have been calculated and   variation of Z components by time have shown in Figure 5.Positive and negative amount for each force mean attractive and repulsive force respect to graphene sheet, respectively. Therefore, up to ~15000 fs positive force is more than negative force which means TC molecule closes to graphene sheet.
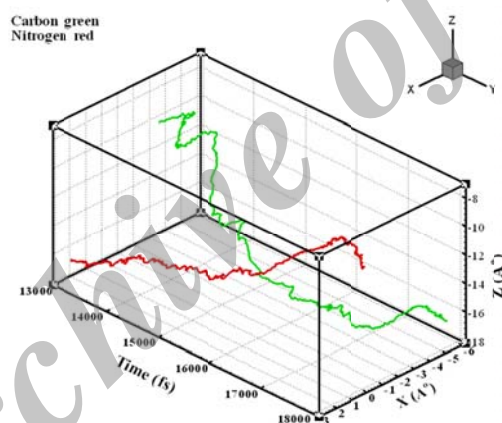

Figure 4: variation of X and Z component by time.

Between ~15000 and ~17000 fs these tow forces are almost equal which is called equilibrium of adsorption. After ~17000 fs repulsive force is dominated and TC molecule goes far away from graphene sheet.
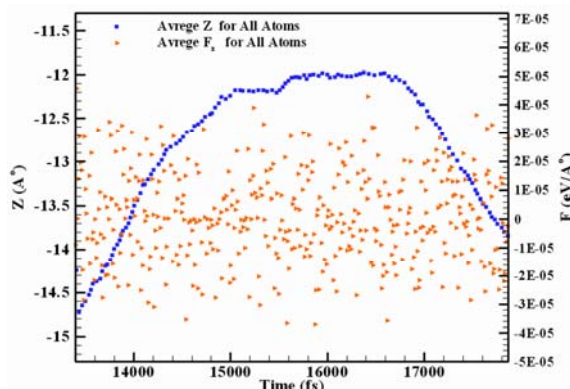
360

Figure 5: variation of X and Z component by time.

4. Conclusion

Due to phenolic ring structure of TC, double bonds and ammine group, TC has appropriate interaction with graphene via π-π stacking. Simulation showed the presence of π–π stacking interactions between TC and graphene's surface. The closest distance between TC and GO was 6.2 Å. After 15000 fs which distance between center of TC and GO sheet was 7 Å, TC started to turn. After 17000 fs, the ammine group side of TC moved far from graphene surface to 5 Å distance. The results indicated that some of the TC molecules were adsorbed and some of them were repulsed by graphene sheet simultaneously which represent the equilibrium concentration. TC molecules were in the mode of adsorption and desorption from graphene surface and the total energy of adsorption and release was equal to -6800 eV. According to LAMMPS instruction, if energy is stronger than -5000 eV, TC molecules attached to graphene as a bonding. Also if energy is weaker than -10000 eV, TC molecules and grapheme sheet separate. In case of positive energy TC molecules and grapheme sheet never close together and system collapses it means system is unstable. For energy between -5000 and -10000 eVsystem is adsorption equilibrium and stable. So, graphenesheet could be a suitableforusing in drug delivery system.

References

[1] Bevelander G.,   Nakahara H., Rolle GK., The effect of tetracycline on the development of the skeletal system of the chick embryo,   Dev Biol. **2**(1960) 298–312.
[2] Brenner D., Shenderova O., Harrison J. A., Stuart S. J., Ni B., Sinnott S., A second-generation reactive empirical bond order (REBO) potential energy expression for hydrocarbonsJ Physics: Condensed Matter, **14** (2002) 783-802.
[3] Hirasch H. A.,   Finland M., Antibacterial Activity of Serum of Normal Subjects after Oral Doses of Demethylchlortetracycline, Chlortetracycline and Oxytetracycline,   Engl N., J Med. **260(22)** (1959) 1099–1104.
[4] http://lammps.sandia.gov - Sandia National Laboratories.
[5] Kay P., Blankwell P.A., Boxall A. B. A., Column studies to investigate the fate of veterinary antibiotics in clay soils following slurry application to agricultural land,   J. Environ. Pollut.**134** (2005) 333–341.
[6] Marcano D. C., Kosynkin D. V., Berlin J. M., Sinitskii A., Sun Z., SlesarevA.r, Alemany L. B., Lu W., and Tour J. M., Improved Synthesis of Graphene Oxide, Nano. **4** (2010) 4806-4814.
[7] Porter L. J., Yip S., Yamaguchi M., Kaburaki H., and Tang M., Empirical Bond-Order Description of Thermodynamic Properties of Crystalline Silicon, J. Appl. Phys. **81** (1997) 96–106.
[8] Rapaport D.C., The Art of Molcular Dynamics Simulation, Cambridge University Press, Cambridge 1995, reprinted 2002.
[9] Sayed M., Jefferson J. H., Walker A. B., and Cullis A. G., Molecular dynamics simulations of implantation damage and recovery in semiconductors, Nucl. Instr. Meth. Phys. Res. B, **102** (1995) 218–222.

[10]Ghadim, E, E.,Manouchehri, F., Soleimani, G.,Hosseini, H.,Kimiagar, S.,Nafisi, S., Adsorption Properties of

Tetracycline onto Graphene Oxide: Equilibrium, Kinetic and Thermodynamic Studies,PLOS ONE. **8** (2013) e79254.

[11] Schmitt H.,   Stoob K., Hamscher G.,   Smit E., Seinen W., Tetracyclines and tetracycline resistance in agricultural soils: microcosm and field studies., Microb. Ecol. **51**(2006) 267-276.

[12] Singh, V., Joung, D., Zhai, L., Das, S., Khondaker, S. I, & Seal, S.,Graphene based materials: Past, present and future, Progress in Materials Science, **56** (2011) 178-271.

[13] Smith R., A semi-empirical many-body interatomic potential for modeling dynamical processes in gallium arsenide,Nucl. Instr. Meth. Phys. Res. B, **67**(1992) 335–339.

[14] Stuart S.J., Tutein A.B., Harrison J.A., A Reactive Potential for Hydrocarbons with Intermolecular Interactions, J Chem Phys. **112** (2000) 6472-6486.

[15] Tersoff , Modeling solid-state chemistry: Interatomic potentials for multicomponent systems J., Phys. Rev. B, 39, no. **8** (1989) 5566–5568.

[16] Zhang Y., Chen B., Zhang L., Huang J., Chen F., Yang Z., Yao J., Zhang Z., Controlled assembly of Fe3O4 magnetic nanoparticles on graphene oxide , Nanoscale, **3** (2011) 1446.

[17] Zhu Y., Murali S.,   Cai W., Li X., Suk JW., Potts JR., et al. Graphene and graphene oxide: synthesis, properties, and applications., Adv Mater. **22** (2010) 3906-24.

[18] Rapaport D.C., The Art of Molcular Dynamics Simulation, Cambridge University Press, Cambridge 1995, reprinted 2002.